Production of individual sheet parts using vaporizing foil actuator forming and a flexible liquid-solid tool

J. Bechler*, L. Dombrowski, H. Dardaei Joghan, M. Hahn, Y.P. Korkolis, A. E. Tekkaya

Institute of Forming Technology and Lightweight Components, TU Dortmund University, Germany
*Corresponding author. Email: Jan.Bechler@iul.tu-dortmund.de

Abstract

Conventional sheet metal forming is inflexible, as each part requires costly punch-and-die tools, usually produced by machining of solid steel. These tools are suitable for large batches but inefficient for individual parts, as the cost per part is high. The aim is to produce individual parts with flexibly applicable tools to also reduce the tool costs per part. The high-speed process of vaporizing foil actuator forming (VFAF) decreases the tool costs by replacing the solid steel punch with a flexible, low-cost, electrically exploding aluminum foil. Until now, also VFAF relies on conventional solid steel dies. This paper investigates the feasibility of a novel flexible liquid-solid tool to manufacture patient-specific cranial implants as an example of highly individual parts. The liquid solid-tool comprises of a thin form-giving additively manufactured (AM) polymer die which is supported by a shear thickening fluid (STF). When the sheet impacts the AM polymer, the STF behaves quasi-solid providing structural die support during forming. The new tool concept also increases the flexibility by potentially reusing a part of the tool – the STF. The results show that the new tool can be designed to successfully manufacture cranial implants with a nominal geometry deviation of ± 1 mm. The deviation lies in the range of other competing flexible processes like powder bed fusion or single point incremental forming. Hence, the liquid-solid tool can replace solid steel dies and decrease the tool costs drastically compared to the solid dies.

Keywords

Vaporizing foil actuator forming, Shear thickening fluid, Individual parts, Flexible tooling

1 Introduction

In conventional sheet metal forming the tools, such as punches and dies, are machined from solid steel and are inherently geometry-bound to one part design. Long lead times make these tools both time- and cost-consuming. While the high costs and extended lead times are usually not critical in mass production, since the expenses are distributed across a large number of parts, resulting in a low tooling cost per unit. However, they become a significant drawback for individual or low-volume production, where the tooling cost per part remains high. In recent years, several attempts were made to replace geometry-bound tools with flexible tools to produce different individual parts with the same tool and thereby decrease the tool costs per part. For example, the rubber pad forming replaces the die with a flexible rubber pad (Afteni et al., 2018). Nakajima (1969) developed a reconfigurable matrix of pins, which can move orthogonally to the tool base, in order to replace both geometry-bound tools. Single point incremental forming (SPIF) entirely avoids the usage of any specific die and punch (Leszak, 1967). However, SPIF has a low geometrical accuracy, partly due to the high elastic springback of the locally formed part, which needs to be taken into account during the process design. In contrast to this, impulse forming processes decrease the elastic springback (Baron and Henn, 1964) due to an elastic (Golovashchenko, 2009) or plastic wave front (Kamal, 2005) which travels through the thickness of the sheet and releases residual stresses and strains. Furthermore, working media- or working energy-based impulse processes replace the punch with a flexibly applicable impulse pressure due to their working principle. However, until now also in impulse forming processes solid steel dies are used. Pegel et al. (2018) showed for electrohydraulic forming, that the steel die can be replaced by a bulk additively manufactured (AM) polymer die, which can resist the impact from the sheet. Later, Hahn et al. (2021) invented a novel flexible liquid-solid tooling concept. There, a thin AM polymer die is refilled with a shear thickening fluid (STF). The STF solidifies upon impact of the sheet, thereby mechanically supporting the thin AM polymer die. A main advantage of this method is the reusability of the STF for other geometries. Hahn et al. (2021) validated this concept for electromagnetic forming (EMF) and showed the necessity of the STF. However, a key limitation of EMF is its reliance on a high electrical conductivity, restricting its applicability to a range of materials. To address this limitation, impulse forming processes that are independent of a material's conductivity, such as vaporizing foil actuator forming (VFAF), can be employed. The VFAF uses an actuator, e.g., an aluminum foil, which is connected to a capacitor bank with a resistance R, an inductance L, and a capacity C. Upon discharge, within a few microseconds, the actuator undergoes resistive heating due to the application of the high voltage $U(t)$ and electrical current $I(t)$, the foil actuator vaporizes leading to an explosive expansion. This rapid expansion generates the impulse pressure $p(t)$ that forms the sheet metal into a form-giving die via an intermediate elastomer layer (**Fig. 1**).

This paper investigates the feasibility of forming an individual part with VFAF and the new liquid-solid tool concept. The individual part is a real-world example of patient specific cranial implants published by Li et al. (2021a) (**Fig. 5 a**)). In the following, the design of the novel tool, including its needed air evacuation, is described. Then, its impact on experimental forming results is analyzed.

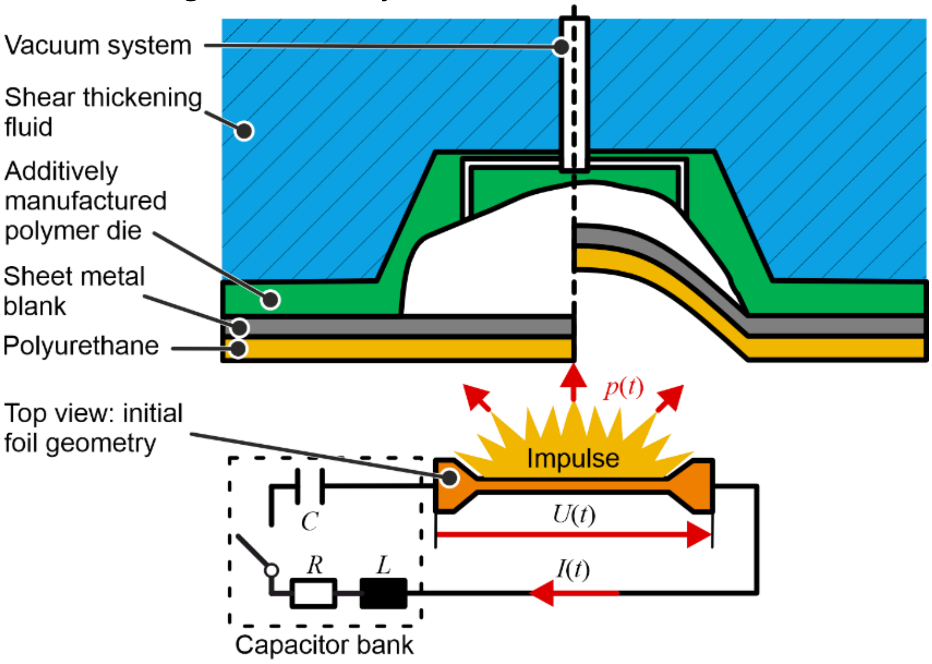

Figure 1: *Schematic principle of the vaporizing foil actuator forming with the new flexible liquid-solid tool concept*

2 Methodology

First, the experimental setup for the part forming is described, along with the method used to evaluate the forming results. Second, the design is presented.

2.1 Experimental setup

Principally the same experimental setup for the VFAF as in Hahn et al. (2019) and for the liquid-solid tool concept as in Hahn et al. (2021) is used. Therefore, only the most important aspects are mentioned here. The actuator is an 0.05 mm thin aluminum foil with a rectangular vaporization area. The foil is insulated with polyamide tape. The vaporization area has dimensions of $b_0 = 18$ mm (x-direction) and $l_0 = 61.7$ mm (y-direction). The longer dimension of the cranial implant is oriented along the vaporization area (y-direction). The energy input deposited until the burst E_b is calculated using MATLAB by analyzing the measured time-dependent voltage $U(t)$ and current $I(t)$ data. The burst energy w_b per vaporized foil mass m, defined as $w_b = E_b / m$, is thus determined. The discharge energy of the capacitor bank is chosen to be $E_{Inp.} = 9.48$ kJ and is kept constant. The measured specific burst energy w_b is an indicator for the forming pressure. The sheet material is titanium grade 2 with a thickness $s = 0.5$ mm. The STF is a cornstarch water suspension with a cornstarch concentration of 55-wt%, which solidifies upon impact, as reported by Crawford et al. (2013). The accuracy of the formed cranial implants is evaluated by scanning the implant using the ATOS Triple Scan system from the company Carl Zeiss AG. The scanned geometries are then compared to the nominal CAD geometry using the 3D analysis software GOM Professional 2020. The minimum and maximum surface deviations δ_{min} and δ_{max} are determined by the normal distance from the nominal CAD geometry to the formed sheet metal.

2.2 Die design

The die is developed using Autodesk Inventor Professional 2024 software, with a patient-specific cranial implant surface from Li et al. (2021b) (Fig. 5 a)) defining the form-giving contour of the die. The target surface for the cranial implant is extrapolated tangentially in the radial direction by 10 mm to prevent discontinuities between the target surface of the implant and the remaining die surface. Preliminary studies were carried out to determine the position of the air evacuation system to withstand the impact of the sheet. Here, only the final design is shown (**Fig. 2 a)**). The air evacuation system is positioned at ± 45° to the vaporization area (**Fig. 2 b)**) with a diameter of d = 2 mm and a minimum die thickness of t_{min} = 12.9 mm. The die is additively manufactured using fused deposition modeling (FDM) with ABS material on an UltiMaker 3. The layer thickness is set to t_s = 0.15 mm and a 100 % infill density is used.

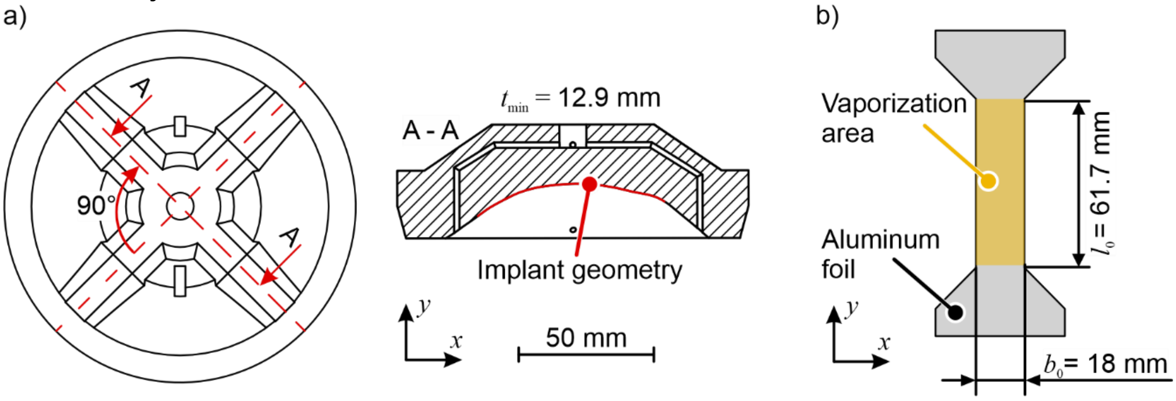

Figure 2: *The position of a) the air evacuation system ± 45° to the x-direction and b) the orientation of the vaporizing foil*

3 Results and Discussion

This section analyzes the geometric accuracy of the formed cranial implant and addresses the influence of the STF.

3.1 Geometric accuracy after VFAF

The maximum and minimum surface deviation from the CAD geometry after forming and before laser cutting is δ_{min} = -0.83 mm and δ_{max} = 0.88 mm (**Fig. 3 a)**). Together with the preliminary experiments (not shown here), the results show a consistent trend where the surface of the formed implant is lower than the nominal CAD geometry (negative deviation) in the direction orthogonal to the vaporization area (*x*-direction), while it is higher (positive deviation) along the vaporization area (*y*-direction).

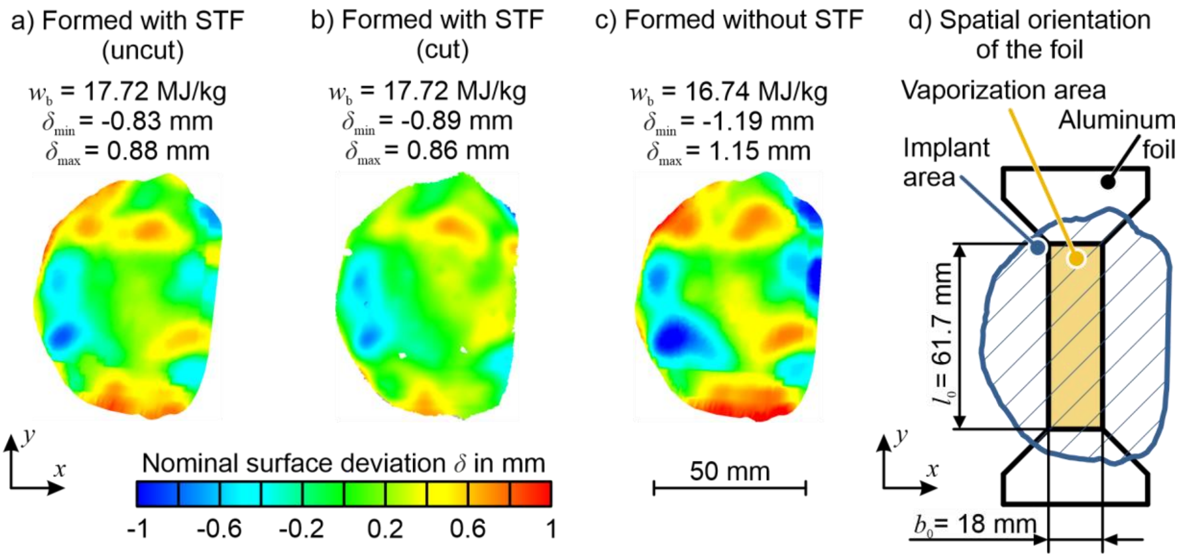

Figure 3: *Nominal surface deviation from the CAD geometry after VFAF a) formed with STF (uncut), b) formed with STF (cut), c) formed without STF and, d) spatial orientation of the foil to the later implant*

One explanation for these deviations is the (burst) pressure distribution. The extended vaporization zone in the longer foil direction, which is the direction of current flow, generates a correspondingly longer pressure pulse in that direction (*y*). This plastically accelerates a larger sheet mass fraction in this direction compared to the direction orthogonal to it (*x*). This causes the die to elastically flex more in the long foil direction than orthogonal to it and thus causes the observed differences in surface deviations. This is supported by numerical simulations, which are beyond the scope of this paper. A possible solution to avoid these inaccuracies could be an equal pressure distribution in both directions. After laser cutting the cranial implant out of the sheet, the minimum surface deviation increases to δ_{min} = - 0.89 mm and the maximum deviation decreases to δ_{max} = 0.86 mm (**Fig. 3 b)**). This change lies within the range of the measuring error, though. The necessity of the STF during VFAF is proven with an additional experiment without STF. The absence of the STF decreases respectively increases the surface deviation to δ_{min} = -1.19 mm and δ_{max} = 1.15 mm (**Fig. 3 c)**). Moreover, the missing structural support during forming causes a horizontal delamination of the AM die (**Fig. 4**), so that it cannot be used for more parts. It is concluded that this horizontal delamination leads to the increased surface deviation due to the lack of structural support. The results thus show the necessity of the STF in maintaining geometric accuracy in VFAF, also for a batch size of just one.

The burst pressure has a significant influence on the surface derivation. Preliminary studies to determine the necessary burst pressure, beyond the scope of this paper, show that if the burst pressure is too low, die contact may not occur, thereby increasing surface deviations and if the burst pressure is too high, it can lead to delamination of the AM die, which also increases surface deviations, as illustrated in Fig. 3c).

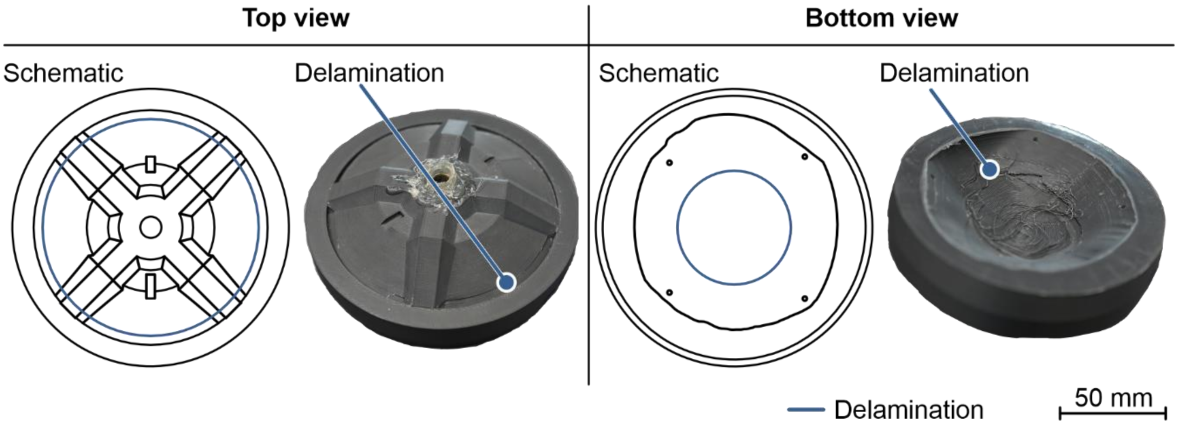

Figure 4: *Visualisation of the AM die failure by delamination of the layers for a part formed without STF*

3.2 Demonstrator

The achieved geometric accuracy of the formed implant (**Fig. 5 b)- c)**) with δ_{min} = -0.89 mm and δ_{max} = 0.86 mm is comparable to that of additively manufactured titanium cranial implants with δ_{min} = -1.11 mm and δ_{max} = 0.42 mm (Ackermann et al., 2019) and even more accurate compared to implants produced via incremental sheet forming with δ_{min} = -2.95 mm and δ_{max} = 1.83 mm (Thakur and Chauhan, 2024). The results show that employing VFAF in combination with the new flexible liquid-solid tool enables a competitive manufacture of individual parts. Furthermore, without addressing detailed calculations, the tool cost for the novel tool concept is 64 % lower compared to a solid steel die and reduces the scrap by 81 vol. % compared to a conventionally machined solid steel die.

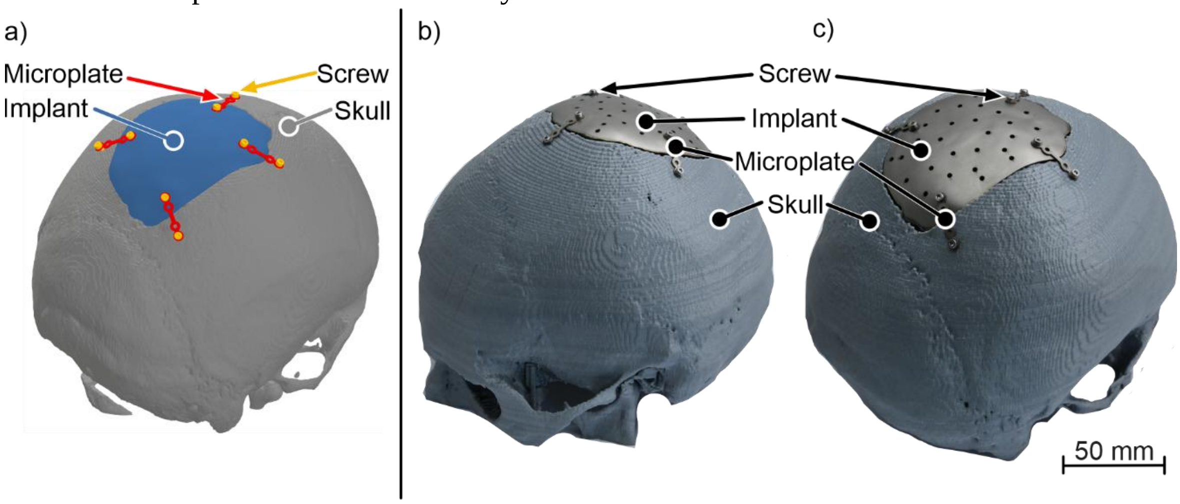

Figure 5: *Patient-specific cranial implant a) nominal geometry b) - c) manufactured by VFAF with the new tool concept (for the data see Li et al. (2021b), Jindal et al. (2023))*

4 Summary and Outlook

This study demonstrates the feasibility of manufacturing individual sheet parts, like patient-specific cranial implants, using VFAF in combination with the flexible liquid-solid tool concept. The usage of AM allows the design of complex air evacuation channels and a quick manufacturing of the polymer die later filled with the needed STF. The geometric accuracy of the formed implants is found to be comparable to that of directly additively manufactured implants and superior to implants produced by incremental sheet forming. In future work, a numerical model of the process that incorporates a fracture criterion for the AM polymer die could reduce the experimental as well as the time effort to design a suitable AM die.

5 References

Ackermann, M., Safka, J., Capek, L., Bobek, J., Mendricky, R., 2019. Selective laser melting technology and individual Ti-6Al-4V implants. MM Science Journal, pp. 2867–2871. https://doi.org/10.17973/MMSJ.2019_06_2018123.

Afteni, C., Costin, G., Iabob, I., Păunoiu, V., & Teodor, V., 2018. A review on sheet metal rubber-pad forming. Annals of" Dunarea de Jos" University of Galati, Fascicle V, Technologies in Machine Building, (36), pp. 49-54.

Baron, H. G., & Henn, R. H., 1964. Spring-back and metal flow in forming shallow dishes by explosives. International Journal of Mechanical Sciences, 6(6), 435-IN5.

Crawford, N. C., Popp, L. B., Johns, K. E., Caire, L. M., Peterson, B. N., & Liberatore, M. W. ,2013. Shear thickening of corn starch suspensions: Does concentration matter?. Journal of colloid and interface science, (396), pp. 83-89.

Golovashchenko, 1999. Numerical and experimental results on pulsed tubes calibration. In Proceedings of the Minerals, Metals & Materials Society (TMS) Annual Meeting "Sheet metal forming technology, M. Demeri ed., San Diego, California, pp. 117-127.

Göttmann, A., Korinth, M., Schäfer, V., Araghi, B. T., Bambach, M., Hirt, G., 2013. Manufacturing of individualized cranial implants using two point incremental sheet metal forming. In Future Trends in Production Engineering: Proceedings of the First Conference of the German Academic Society for Production Engineering (WGP), Berlin, Germany, pp. 287-295. Springer Berlin Heidelberg. https://doi.org/10.1007/978-3-642-24491-9_28.

Hahn, M., Goyal, S., Gies, S., & Tekkaya, A. E., 2019. Numerical modeling of energy deposition for vaporizing foil actuator forming. In proceedings of the 13th International Conference on Numerical Methods in Industrial Forming Processes-NUMIFORM, Portsmouth (NH), USA.

Hahn, M., Kumar, V., Tekkaya, A.E, 2021. Impact activated fluid-sloid tool: towards more flexible high speed forming. International Conference on High speed Forming (ICHSF) 2021 (held online). Based on patent DE 10 2020 006 753.0, 2020.

Jindal, P., Chaitanya, Bharadwaja, S. S. S., Rattra, S., Pareek, D., Gupta, V., Breedon, P., Reinwald, Y., Juneja, M., 2023. Optimizing cranial implant and fixture design using different materials in cranioplasty. Proceedings of the Institution of Mechanical Engineers, Part L: Journal of Materials: Design and Applications, (237), pp. 107-121. https://doi.org/10.1177/14644207221104875.

Kamal, M., 2005. A Uniform Electromagnetic Actuator for Forming Flat Sheets, Doctoral dissertation, Ph. D. thesis, Ohio State University, Columbus.

Leszak, E., 1967. Apparatus and Process for Incremental Dieless Forming. U.S. Patent 3342051A1.

Li, J., Krall, M., Trummer, F., Memon, A.R, Pepe, A., Gsaxner, C., Jin, Y., Chen, X., Deutschmann, H., Zefferer, U., Schäfer, U., Campe, G. von, Egger, J., 2021a. MUG500+: Database of 500 high-resolution healthy human skulls and 29 craniotomy skulls and implants. Data in brief, (39), 107524. https://doi.org/10.1016/j.dib.2021.107524.

Li J., Krall, M., Trummer, F., Memon, A.R, Pepe, A., Gsaxner, C., Jin, Y., Chen, X., Deutschmann, H., Zefferer, U., Schäfer, U., Campe, G. von, Egger, J., 2021b. MUG500+ Repository. Figshare, 2021. DOI: 10.6084/m9.figshare.9616319

Moiduddin, K., Mian, S.H, Umer, U., Alkhalefah, H., 2019. Fabrication and Analysis of a Ti6Al4V Implant for Cranial Restoration. Applied Sciences, (9), 2513. https://doi.org/10.3390/app9122513.

Nakajima, N., 1969. A newly developed technique to fabricate complicated dies and electrodes with wires. Bulletin of Japan Society of Mechanical Engineers, 12(54), pp. 1546-1554.

Pegel H, Langstädtler L, Herrmann M, Schenck C, Kuhfuss B., 2018. Electrohydraulic sheet metal forming with flexible tools. MATEC Web Conf. 2018;190:12001. https://doi.org/10.1051/matecconf/201819012001.

Thakur, S., Chauhan, S.R, 2024. Patient-Specific Cranial Implant Fabrication: Evaluating Single-Point Incremental Forming with Perforated Titanium Grade-2 Sheets. J. of Material Engineering and Performance, pp. 1-11. https://doi.org/10.1007/s11665-024-09633-x.